Journal of Magnetic Resonance **151,** 320–327 (2001)
doi:10.1006/jmre.2001.2354, available online at http://www.idealibrary.com on IDEAL®

COMMUNICATIONS

^{1}H–^{1}H MAS Correlation Spectroscopy and Distance Measurements in a Deuterated Peptide

B. Reif,[1] C. P. Jaroniec, C. M. Rienstra,[2] M. Hohwy,[3] and R. G. Griffin[4]

Department of Chemistry and MIT/Harvard Center for Magnetic Resonance, Francis Bitter Magnet Laboratory, Massachusetts Institute of Technology, Cambridge, Massachusetts 02139

Received November 9, 2000; revised April 10, 2001; published online July 5, 2001

In this Communication, we demonstrate the use of deuteration together with back substitution of exchangeable protons as a means of attenuating the strong ^{1}H–^{1}H couplings that broaden ^{1}H magic angle spinning (MAS) spectra of solids. The approach facilitates ^{15}N–^{1}H correlation experiments as well as experiments for the measurement of ^{1}H–^{1}H distances. The distance measurement relies on the excellent resolution in the ^{1}H MAS spectrum and homonuclear double quantum recoupling techniques. The ^{1}H–^{1}H dipolar recoupling can be analyzed in an analytical fashion by fitting the data to a 2- or 3-spin system. The experiments are performed on a sample of the dipeptide N–Ac–Val–Leu–OH, which was synthesized from uniformly [^{2}H, ^{15}N] labeled materials and back-exchanged in H_2O.

INTRODUCTION

The high gyromagnetic ratio of protons renders these nuclear spins the ideal candidate for detection and measurement of long-range distances. They are, however, not generally used in solid-state NMR experiments due to the fact that multiple ^{1}H–^{1}H dipolar couplings lead to homogeneously broadened spectral lines that are not narrowed by magic angle spinning (MAS). Furthermore, the strong ^{1}H–^{1}H dipolar couplings attenuate the weaker, structurally interesting long-range interactions. Specifically, these strong couplings lead to truncation effects (*1, 2*) that make accurate ^{1}H–^{1}H distance determinations problematic.

Several approaches are employed to address these problems. Initially, homonuclear decoupling techniques, such as WAHUHA, MREV-8, and CRAMPS (*3–5*), were used to average the homonuclear dipolar interactions. These techniques are restricted to relatively slow spinning frequencies and scale the chemical shift leading to a smaller effective dispersion of the resonances. A second approach utilized recently is based on MAS at high Larmor and spinning frequencies (*6, 7*) and yields an advantage in sensitivity compared to the low-γ nucleus detected version of the experiment. However, only correlation spectra with semi-quantitative information on ^{1}H–^{1}H interactions can be obtained in this approach.

In principle, ^{1}H spin dilution can provide another approach to increase the resolution of ^{1}H spectra. The idea of using spin dilution in solid-state spectra was explored initially by randomly diluting ^{1}H to ∼1 mole % in a ^{2}H lattice. Experiments were first performed on static samples with ^{2}H decoupling (*8, 9*) and more recently with MAS techniques (*10, 11*), where the ^{2}H decoupling was not necessary because of the sample rotation. Concurrently, the dilution to ∼1% decreased the sensitivity and lengthened the spin-lattice relaxation time of the remaining protons. However, it was possible to partially circumvent these problems by cross polarization from ^{2}H to ^{1}H (*11*). In this communication, we present spectra from ^{1}H spins diluted in a well-defined manner. In particular, exchangeable ^{1}H–^{15}N sites are fully protonated by back exchange, whereas all other sites are perdeuterated. This approach permits ^{1}H detection with very high sensitivity, ^{15}N–^{1}H correlation spectroscopy with well-resolved ^{1}H resonance lines, and ^{1}H–^{1}H distance measurements. Since long-range distance constraints are very useful in determining the three-dimensional fold of a protein, the measurement of these dipolar couplings could be of importance in structural studies of larger biomolecules. A large number of assignment techniques have been developed and recently applied to small proteins (*12, 13*). However, a general method to determine the global fold of a protein in the solid-state has not yet been established. The present approach is a step in this direction.

[1] Current address: Institut für Organische Chemie und Biochemie, Technische Universität München, Lichtenbergstr. 4, D-85746 Garching, Germany.

[2] Current address: Department of Chemistry, Columbia University, New York, New York 10027.

[3] Institute for Molecular Biology and Biophysics, ETH Honggerberg HPK G2, CH-8093 Zürich, Switzerland.

[4] To whom correspondence should be addressed. E-mail: griffin@ccnmr.mit.edu or rgg@mit.edu.

1090-7807/01 $35.00

RESULTS

^1H–^{15}N Correlation Spectroscopy

Figure 1 shows a comparison of the 1D ^1H spectra of the dipeptide N–Ac–Val–Leu–OH recorded at $\omega_r/2\pi = 12.5$ kHz. The signal-to-noise ratio of the ^1H detected experiment is 2000 : 1, as compared to 83 : 1 in the corresponding ^{15}N detected 1D CP experiment. Taking into account a transfer efficiency of ca. 56% in the CP transfer step, the ratio of signal intensities between ^1H and ^{15}N detected experiments is ~13.5. The theoretical achievable maximum for the magnetization transfer corresponds to $(\gamma_H/\gamma_N)^{3/2} = 31.0$, assuming the same efficiency for both nuclei. The ^1H linewidth in these experiments, is determined by the residual dipolar interactions among the dilute proton spins, and is governed by a $1/\omega_r$ spinning frequency dependence at higher MAS rates (*40*, *41*).

Care must be taken during decoupling of the proton spins while detecting ^{15}N (Fig. 2). The spin system approximates an ensemble of isolated spin pairs. Homonuclear ^1H–^1H flip-flop terms in the Hamilton operator of the dipolar interaction, which lead to a narrowing of the ^{15}N spin resonance (*14*), are much smaller than in the case of a fully protonated peptide. Application of the TPPM (*15*) decoupling sequence is essential (*16, 17*) to achieve narrow resonance lines as is illustrated in Fig. 2. The assignment of the ^{15}N resonances in N–Ac–Val–Leu–OH was performed on a uniformly ^{13}C,^{15}N-labeled sample, using RFDR (*18, 19*) and 2D DCP (*20*) type experiments (*21*).

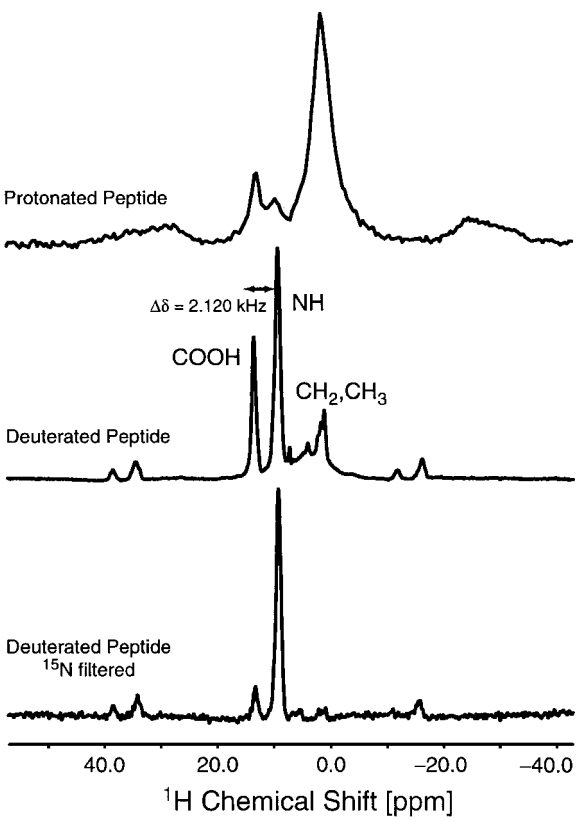

FIG. 1. Comparison of the 1D ^1H spectra of N–Ac–Val–Leu–OH ($\omega_r/2\pi = 12.5$ kHz): fully protonated peptide (top), deuterated peptide displaying only exchangeable protons (middle), deuterated peptide after application of a ^{15}N filter, showing only protons strongly coupled to ^{15}N (bottom). Eight scans were recorded for each experiment. Optimal signal-to-noise ratio was achieved with a recycle delay of 11.0 s.

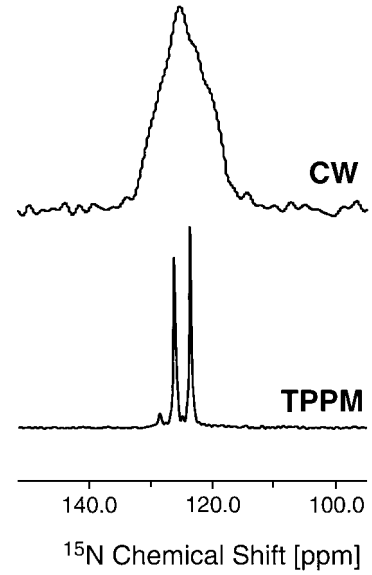

FIG. 2. One dimensional ^{15}N spectra with CW (top) and TPPM (bottom) decoupling of [^2H,^{15}N]N–Ac–Val–Leu–OH; in both cases the rotor frequency and the decoupling ^1H rf field have been set to $\omega_r/2\pi = 12.5$ kHz and $\omega_{rf}(^1H)/2\pi = 62.5$ kHz, respectively. Eight scans were recorded for each experiment with a recycle delay of 11.0 s.

Figure 3 compares ^{15}N–^1H correlation spectra recorded on a protonated and deuterated sample of ^{15}N labeled N–Ac–Val–Leu–OH. In the deuterated sample, with a cross polarization mixing time of 0.15 ms, only correlations between the amide protons and the nitrogen are observed. For longer CP times (>1 ms), a correlation between the valine nitrogen and the leucine carboxyl hydrogen can also be detected. This is in agreement with the X-ray structure (*22*) where the valine amide proton is hydrogen bonded to the leucine carboxyl group (Fig. 4). For the protonated sample, correlations between the amide nitrogen and all hydrogens are observed. At a spinning frequency of 12.5 kHz, the ^1H resonance line has a FWHM of 272 Hz for the leucine, and 322 Hz for the valine amide proton for the deuterated peptide, whereas in the protonated sample, the ^1H line width is approximately 1.7 kHz for both resonances. We have observed differences in the ^{15}N chemical shifts for the protonated and perdeuterated N–Ac–VL–OH samples (cf. Fig. 3). (No significant differences were observed in the ^{13}C chemical shifts of the two peptides.) The differences are larger than can be accounted for by isotope effects alone (*23*). This indicates possible differences in the quality of the two samples.

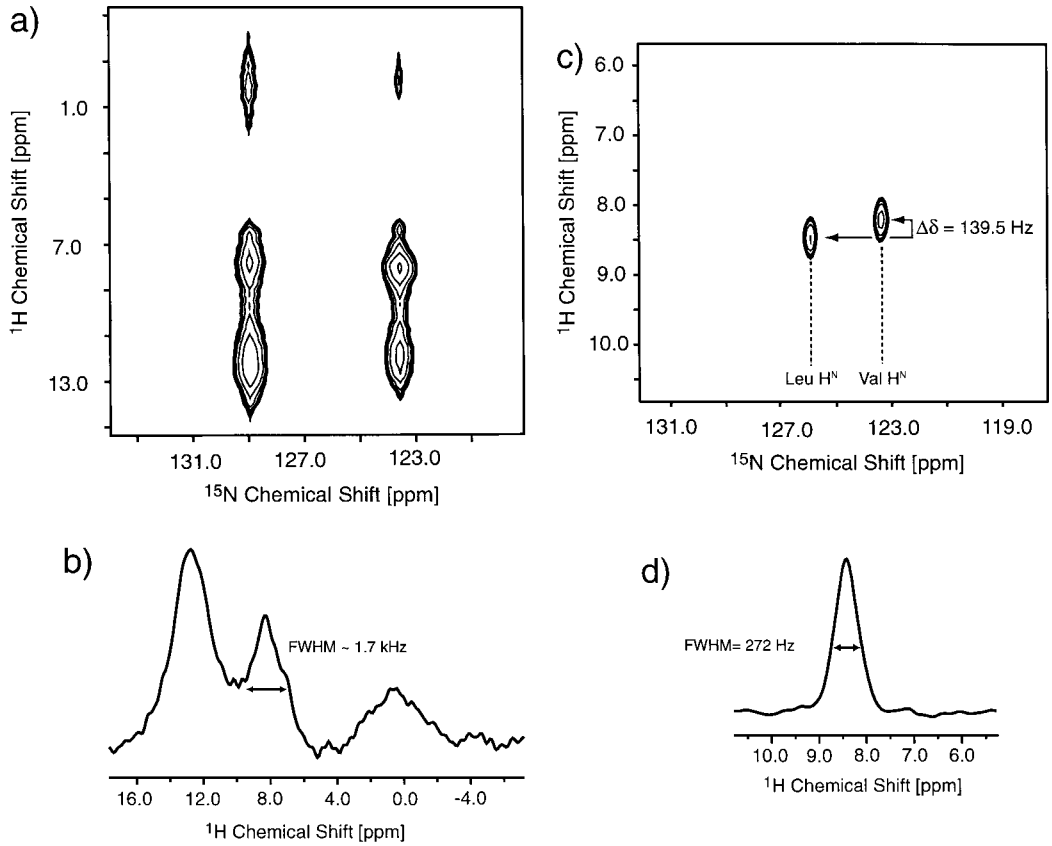

FIG. 3. 2D ^{1}H,^{15}N–HETCOR spectra for the protonated and deuterated N–Ac–Val–Leu–OH sample. In both experiments, magnetization is transferred from protons to nitrogens via CP. A ^{15}N π-pulse in the middle of the ^{1}H evolution period (total increment $\Delta = 2n\tau_r$) was used to refocus the ^{1}H–^{15}N scalar coupling. (a) 2D spectrum and (b) 1D trace along the ^{1}H dimension (leucine) for the protonated N–Ac–Val–Leu–OH sample. The cross-polarization mixing time was set to 2.0 ms, the TPPM decoupling level was adjusted to 95.0 kHz. (c) 2D spectrum and (d) 1D trace along the ^{1}H dimension (leucine) for the perdeuterated N–Ac–Val–Leu–OH sample. The cross-polarization mixing time was set to 0.15 ms; the TPPM decoupling power was adjusted to 62.5 kHz. The ^{1}H resonance linewidth is on the order of 1.7 kHz and 272 Hz for the leucine amide proton in the protonated and deuterated samples, respectively.

^{1}H–^{1}H Distance Measurements

Important constraints for the global fold of a protein can be obtained by measuring long distances. These structurally constraining distances are ideally measured via correlations between high-γ nuclei, due to the dependence of the dipolar coupling on the gyromagnetic ratio. In principle, ^{1}H–^{1}H correlations permit determination of distances up to 16 Å (*24*). In fully protonated samples, however, the information is attenuated by strong dipolar ^{1}H–^{1}H couplings which make it impossible to use protons for direct long-range transfers. This effect is referred to as dipolar truncation (*1*, *2*) and has been demonstrated on uniformly ^{13}C-labeled molecules. A similar effect is observed in solution-state NMR (*25*) where the presence of strong scalar couplings attenuates magnetization transfer involving weaker interactions. Proton spin dilution circumvents this problem by retaining only the weaker dipolar couplings that are structurally interesting. In deuterated samples, according to the protocol of the sample preparation, only protons that exchange with the solvent protons are retained. Double quantum recoupling techniques have been used extensively for correlation spectroscopy (*2*, *26*) and projection angle experiments (*27*) to determine torsion and projection angles in uniformly ^{13}C,^{15}N labeled peptides. Homonuclear distance measurements have been performed primarily on selectively labeled samples (*28–34*). Only recently, these techniques were adapted for uniformly ^{13}C,^{15}N-labeled samples (*35*, *36*).

In order to measure ^{1}H–^{1}H distances, the homonuclear ^{1}H–^{1}H dipolar interaction is recoupled by application of the CMR7 (*26*) sequence, which is a γ-encoded multiple pulse sequence (*37*). CMR7 exhibits a broad bandwidth that provides excellent compensation for phase transients and rf inhomogeneity and is relatively insensitive to chemical shift anisotropy. The first order average Hamiltonian $H^{(1)}$ of the homonuclear interaction of a n-fold pulse sequence CN_n^v which is constructed from N elements within n rotor periods can be expressed as (*38*)

$$H_{IS}^{(1)} = \frac{1}{N}\sum_{p=0}^{N-1}\sum_{m=-2}^{+2}\sum_{\mu=-2}^{+2}\overline{\omega_{\mu,m}^{IS}}\exp\left[i\frac{2\pi}{N}(\mu+mn)p\right]T_{2,\mu}^{IS} \quad [1]$$

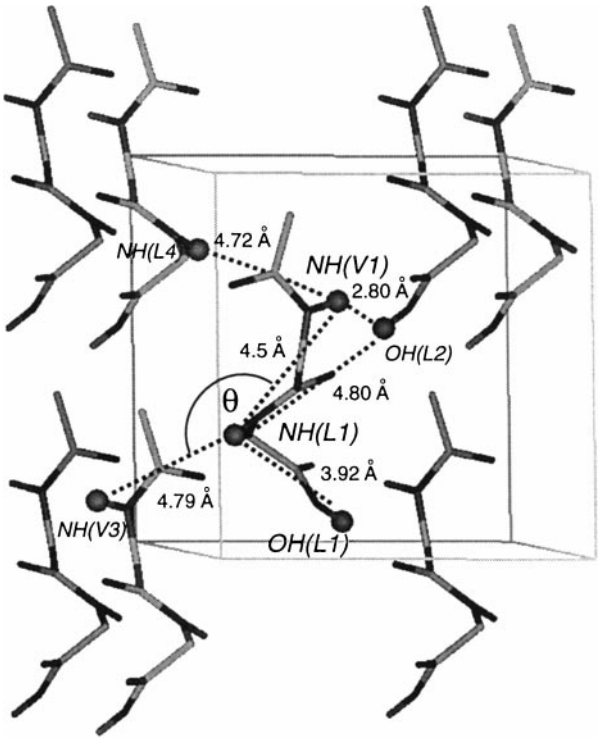

FIG. 4. Structure of N–Ac–Val–Leu–OH in the crystal unit cell (*22*). All ^{1}H–^{1}H distances between exchangeable protons within one molecule, as well as ^{1}H–^{1}H distances between exchangeable protons in adjacent molecules in different unit cells within 6.0 Å are indicated. For simplicity, only distances originating from one molecule in the unit cell are shown. Furthermore, all nonexchangeable protons, as well as all side chains, are omitted for clarity. Crystals have $P2_1$ monoclinic symmetry. The dimensions of the unit cell are $a = 9.458$ Å, $b = 9.523$ Å, $c = 9.409$ Å, $\alpha = 90°$, $\beta = 114.55°$, $\gamma = 90°$.

with

$$\overline{\omega^{IS}_{\mu,m}} = \frac{N}{n\tau_r} \int_0^{\frac{N}{n\tau_r}} d\tau\, i^{\mu} \omega^{IS}_{0,m} d^2_{\mu,0}[\beta_{r.f.}(\tau)] e^{i\mu\alpha_{r.f.}(\tau)} e^{im\omega_r\tau}. \quad [2]$$

The nomenclature for the irreducible tensor operators and spatial operators follows the convention in Ref. (*1*). Recoupling occurs at $\mu + nm = qN$. Choosing $N = 7$ and $n = 2$ yields recoupling of the spatial component $\omega^{(m=\pm1)}$. Since CMR7 is a γ-encoded sequence, the amplitude of the recoupled interaction is only dependent on the crystallite β-angle. Therefore, the efficiency of double quantum excitation between spins i and j in a 2-spin system can be described analytically as a function of the incremented double quantum excitation time t_1 (without inclusion of differential relaxation between the spin states $I_z^{(14)}$ and $I_\gamma^{(14)}$),

$$DQ_{ij}(t_1) = \int_0^{\pi} d\beta_{ij} \sin\beta_{ij} \sin^2(|\kappa|\tilde{b}_{ij}t_1) \exp\left(-2R_2^{DQ}t_1\right), \quad [3]$$

where the orientation dependent dipolar coupling $\tilde{b}_{ij}$ between spins i and j is

$$\tilde{b}_{ij} = b_{ij} \sin 2\beta_{ij} = \frac{\mu_0}{4\pi} \frac{\gamma_i\gamma_j\hbar}{r_{ij}^3} \sin 2\beta_{ij}. \quad [4]$$

The scaling factor of the CMR7 pulse sequence, κ, is equal to 0.232 (*26*), and R_2^{DQ} corresponds to the effective relaxation rate during the double quantum excitation period. β_{ij} is the crystallite β-angle for the dipolar interaction between spins i and j. In the N–Ac–Val–Leu–OH sample, where only exchangeable sites are protonated, the amide proton of valine is hydrogen bonded and therefore in close spatial proximity (2.80 Å) to the carboxyl proton of a leucine residue in a neighboring molecule as illustrated in Fig. 4. Typical values for the corresponding ^{1}H–^{1}H corresponding distances and scaled ^{1}H–^{1}H dipolar interactions in this system are 2.80 Å (1269.5 Hz, NH(V1)–OH(L2)), 3.92 Å (462.6 Hz, NH(L1)–OH(L1)), 4.50 Å (305.8 Hz, NH(V1)–NH(L1)), and 4.79 Å (253.6 Hz, NH(V3)–NH(L1)).

Figure 5a depicts the pulse sequence for the 3D-DQ{^{1}H,^{1}H}–^{15}N correlation experiment. Starting from equilibrium magnetization, ^{1}H–^{1}H double quantum coherence is excited during t_1, evolves during t_2, and is reconverted to longitudinal magnetization. We employ the CMR7 multiple pulse sequence for this process. Figure 5b illustrates a representative 2D slice ($t_1 = 0.448$ ms) from the 3D-DQ{^{1}H,^{1}H}–^{15}N correlation experiment. Connectivities between an amide proton and another amide proton or carboxyl hydrogen, respectively, for leucine and valine are indicated. Figure 6 shows experimental and simulated data for a slice through a {H^N, H^N} double quantum cross peak in the 3D-DQ{^{1}H,^{1}H}–^{15}N experiment, detected on the valine (filled circles) and leucine (triangles) amide nitrogen. Application of a double quantum filter yields a sinusoidally modulated signal. The ^{1}H–^{1}H DQ buildup curve for valine can be fit well by a 2-spin approximation dominated by the [NH(V1)–OH(L2)] coupling and assuming a scaled dipolar coupling of 1180 Hz, a double quantum relaxation constant R_2^{DQ} of 620 Hz and an amplitude scaling factor of 62% (for γ-encoded recoupling sequences the maximum achievable double quantum filtering efficiency is 73% corresponding to an amplitude scaling factor of 100%). A scaled dipolar coupling of 1180 Hz is equivalent to a ^{1}H–^{1}H distance of 2.87 Å. This is in agreement with the distance of 2.80 Å found in the X-ray structure. The fitted value for R_2^{DQ} also compares well with the experimentally determined ^{1}H linewidth of 320 Hz at this spinning frequency.

For the analysis of the ^{1}H–^{1}H double quantum signal, detected on the leucine amide nitrogen, a 2-spin approximation is not sufficient. In fact, even a full simulation including up to five spins does not yield a satisfactory description of the experimental observations for long double quantum excitation times. However, the initial rate buildup of double quantum coherence can be approximated using the analytical relation for

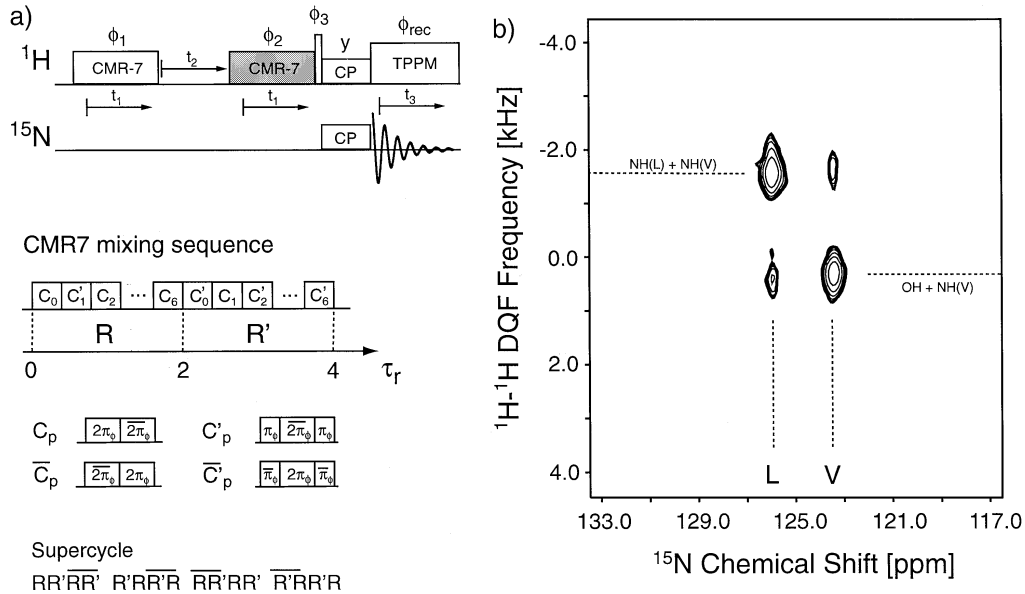

FIG. 5. 3D-DQ{^{1}H,^{1}H}–^{15}N correlation experiment. (a) Pulse sequence. ^{1}H–^{1}H double quantum coherences are excited and reconverted during t_1. DQ chemical shift evolves during t_2. After double quantum excitation, ^{1}H magnetization is reconverted to longitudinal magnetization and transferred to ^{15}N for detection during t_3. DQ filtration is achieved by phase cycling following standard procedures (*42*). CMR7 (*26*) is used for DQ excitation and reconversion. The details of the pulse sequence, as well as the supercycle, are indicated on the bottom of the figure. (b) 2D-Spectrum of the 3D-DQ{^{1}H,^{1}H}–^{15}N correlation experiment for [^{2}H,^{15}N]–N–Ac–Val–Leu–OH recorded at $t_1 = 0.448$ ms and $\omega_r/2\pi = 8.928$ kHz. The ^{1}H 90° pulse length in the CMR7 multiple pulse sequence was set to 4.0 μs to accommodate seven C-elements in two rotor periods. The CMR7 ^{1}H–^{1}H dipolar recoupling period during t_1 was incremented in steps of complete CC' elements (64.0 μs), and a total of 14 experiments were recorded in t_1. In the DQ{^{1}H,^{1}H} chemical shift evolution period t_2, 8 increments were recorded, with an increment of 112.0 μs per experiment yielding a spectral width of 8.928 kHz. The recycle delay between each two transients was set to 11 s and 64 scans were accumulated for each FID, yielding a total experimental time for the 3D experiment of 44 h. TPPM decoupling was used in the direct evolution period, with a ^{1}H rf field of about 62.5 kHz. The CP time was set to 0.15 ms.

The ^{2}H,^{15}N-labeled amino acids valine and leucine were from Cambridge Isotope Laboratories (Andover, MA). Synpep (Dublin, CA) performed the synthesis of N–Ac–VL. The NMR spectra were recorded at an ^{1}H Larmor frequency of 500.0 MHz, using a custom-designed spectrometer and data acquisition software courtesy of Dr. D. J. Ruben. The custom-designed triple resonance transmission line probe was equipped with a 4-mm Chemagnetics (Fort Collins, CO) MAS spinning module. The spinning frequency was controlled to within ±5 Hz using a Doty Scientific (Columbia, SC) spinning frequency controller.

a 3-spin system, derived by Hohwy *et al.* (*2*). The excitation time dependent intensity of a double quantum signal between spins i and j—when spins i, j, and k are dipolar coupled— for a γ-encoded sequence is given as

$$DQ_{ij}(t_1) = \int_0^\pi d\beta \sin\beta \frac{1}{4r^4}\left\{\tilde{b}_{ij}^2 \cos(rt_1)\left[\tilde{b}_{ik}^2 + \left(\tilde{b}_{kj}^2 + \tilde{b}_{ij}^2\right)\cos(rt_1)\right]\sin^2(rt_1)\right\} \quad [5]$$

with

$$r = \sqrt{\tilde{b}_{ij}^2 + \tilde{b}_{ik}^2 + \tilde{b}_{kj}^2}, \quad [6]$$

where $\tilde{b}_{ik}$, $\tilde{b}_{kj}$ are the dipolar coupling constants and β_{ik}, β_{kj} the crystallite β-angles for the dipolar interaction between spins i and k and between spins k and j, respectively. Expansion of the sine and cosine functions for small time arguments yields

$$DQ_{ij}(t_1) = \int_0^\pi d\beta \sin\beta\, 4\tilde{b}_{ij}^2 t_1^2 \left\{1 - t_1^2\left(r^2 - \frac{\tilde{b}_{ik}^2}{2}\right) + \cdots\right\} \quad [7]$$

To first order, this expression is independent of the size and orientation of the passive couplings $\tilde{b}_{ik}$, $\tilde{b}_{kj}$. Numerical simulations show that the first term in Eq. [7] is equivalent to the exact time-dependent buildup of double quantum coherence as given by the formula in Eq. [5] for a 3-spin system in the initial rate regime, and therefore sufficient to describe the initial rate of the double quantum buildup. Higher order terms can be neglected if double quantum excitation times are considered that are small compared to the inverse of the largest coupling involved. Furthermore, the size of the passive couplings must be smaller or of the same order of magnitude as the active coupling of interest. This condition is satisfied in deuterated samples where only the exchangeable sites are protonated. In the present case, one leucine amide proton is dipolar coupled to two valine amide protons, at 4.50 Å and 4.79 Å distance. In order

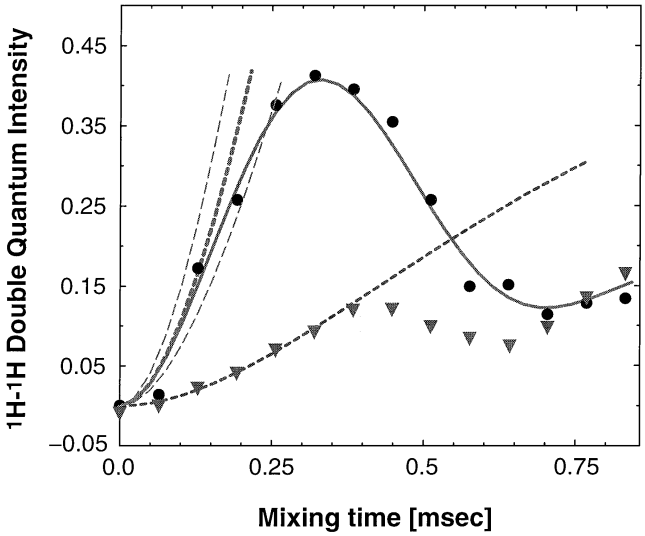

FIG. 6. Experimental and simulated DQ{^{1}H,^{1}H}–^{15}N CMR7 buildup curves for [^{2}H,^{15}N]N–Ac–Val–Leu–OH for valine (filled circles) and leucine (triangles). The figure shows slices along t_1 through the DQ{H^N–H^N} cross peak NH(V)–OH(L) and NH(L)–NH(V) in the 3D-DQ{^{1}H,^{1}H}–^{15}N correlation experiment, detected on the respective amide nitrogens. The experimental data for valine and leucine can be fit using a 2-spin and an initial rate 3-spin approximation, respectively. Fit parameters for valine and leucine are $b_{\mathrm{Val1-NH,Leu2-OH}} = 1180$ Hz, $R_2^{\mathrm{DQ}} = 620$ Hz, and $b_{\mathrm{Leu1-NH,Val1/3-NH}} = 325$ Hz and 252 Hz, $\theta = 125^\circ$, $R_2^{\mathrm{DQ}} = 620$ Hz. The dashed lines for the buildup of the NH(V1)–OH(L2) cross peak indicate the best fit for the initial rate buildup, together with simulations displaying a variation of the size of the dipolar coupling of 17% (corresponding to distances 2.72 Å, 2.87 Å, and 3.05 Å). An amplitude scaling factor of 62% has been used in all simulations. As a reference, the first point of an experiment without double quantum filtration that yields a cosinusoidal oscillation has been used.

to simulate the dipolar dephasing behavior, the size of the two couplings and the angle between the two dipolar vectors must be incorporated into the numerical simulations. Therefore, we express the second β-angle as a function of the included angle. The projection angle and the respective β-angle are related by (*39*)

$$\cos\beta_{ik} = \cos\beta_{ij}\cos\theta_{ij,ik} - \sin\beta_{ij}\sin\theta_{ij,ik}\cos\phi. \qquad [8]$$

Simulations yield optimal fits for the leucine ^{1}H–^{1}H DQ buildup curve, if we assume scaled dipolar couplings of 325 Hz and 252 Hz, respectively, an angle of 125° between the dipolar interactions, a double quantum relaxation constant R_2^{DQ} of 620 Hz, and a scaling factor of 62%. The size of the couplings (325 Hz ≡ 4.41 Å, 252 Hz ≡ 4.80 Å) corresponds well to the distances (4.50 Å, 4.79 Å) found in the X-ray structure for the dipeptide (Fig. 4).

DISCUSSION

The proton linewidths observed in the HETCOR experiments for leucine and valine with $\omega_r/2\pi = 12.5$ kHz are 272 and 320 Hz, respectively. Since the linewidths exhibit a ω_r^{-1} spinning frequency dependence characteristic of an inhomogeneous system (*40, 41*), then the resulting linewidth will be on the order of 90 Hz at a spinning frequency of 35 kHz. Assuming a dispersion of ca. 3.5 ppm for the amide proton resonances in a typical peptide or protein yields sufficient spectral resolution to make the ^{1}H dimension useful in correlation experiments for medium-sized peptides and proteins in solid-state MAS spectra.

As is evident from Fig. 1, the degree of deuteration of the peptide is not complete. Integration of the spectrum suggests that the deuteration percentage is approximately 95%. In the current ^{1}H–^{1}H distance evaluation, no correction from the aliphatic proton background has to be taken into account, since only the buildup of {H^N, OH} or {H^N, H^N} double quantum coherences is considered. The influence of amide protons which are >6.0 Å from the proton under consideration can, however, be neglected. The scaled dipolar coupling for these protons is smaller than 120 Hz and does not influence the initial rate behavior of the double quantum coherence buildup. These longer-range dipolar couplings are reflected in deviations between experimental data and simulations for double quantum excitation times larger than 0.75 ms.

The dipeptide N–Ac–Val–Leu–OH can be considered a model system for a ^{2}H-labeled protein, since the ^{1}H density among molecules in different unit cells is similar to the ^{1}H densities found in larger proteins. Further work in this direction is in progress in our laboratory.

CONCLUSION

In conclusion, we have shown that amide ^{1}H spins in a perdeuterated peptide can be used in MAS solid-state NMR for correlation spectroscopy, yielding high-resolution ^{1}H resonance lines. Further, the ^{1}H spin system is sufficiently dilute to allow the determination of medium-range distances between exchangeable protons in a highly deuterated environment. We believe this approach may be valuable for the determination of the three-dimensional structure of larger fully labeled peptides and proteins.

ACKNOWLEDGMENTS

This research was supported by the NIH Grants AG-14366, GM-23403, and RR-00995. B. R. acknowledges support from the Deutsche Forschungsgemeinschaft (Grant Re1435). C. P. J. is a recipient of a NSF Predoctoral Fellowship.

REFERENCES

1. K. Schmidt-Rohr and H. W. Spiess, "Multidimensional Solid-State NMR and Polymers," Academic Press, London (1994).
2. M. Hohwy, C. M. Rienstra, C. P. Jaroniec, and R. G. Griffin, Fivefold symmetric homonuclear dipolar recoupling in rotating solids: Application

to double quantum spectroscopy, *J. Chem. Phys.* **110,** 7983–7992 (1999).

3. B. Schnabel, U. Haubenreisser, G. Scheler, and R. Müller, 19th Congress Ampere, Heidelberg, 1976, pp. 441.
4. B. C. Gerstein, C. Chow, R. G. Pembleton, and R. C. Wilson, Utility of pulse nuclear magnetic resonance in studying protons in coals, *J. Phys. Chem.* **81,** 565–570 (1977).
5. M. Hohwy, J. T. Rasmussen, P. V. Bower, H. J. Jakobsen, and N. C. Nielsen, ^{1}H chemical shielding anisotropies from polycrystalline powders using MSHOT-3 based CRAMPS, *J. Magn. Reson.* **133,** 374–378 (1998).
6. I. Schnell, A. Lupulescu, S. Haffner, D. E. Demco, and H. W. Spiess, Resolution enhancement in multiple-quantum MAS NMR spectroscopy, *J. Magn. Reson.* **133,** 61–69 (1998).
7. Y. Ishii and R. Tycko, Enhancement in solid state ^{15}N NMR by indirect detection with high-speed magic angle spinning, *J. Magn. Reson.* **142,** 199–204 (2000).
8. A. Pines, D. J. Ruben, S. Vega, and M. Mehring, New approach to high resolution proton NMR in solids: Deuterium spin decoupling by multiple quantum transitions, *Phys. Rev. Lett.* **36,** 110–112 (1976).
9. A. Pines, S. Vega, and M. Mehring, NMR double quantum spin decoupling in solids, *Phys. Rev. B* **18,** 112–125 (1978).
10. A. E. McDermott, F. J. Creuzet, A. C. Kolbert, and R. G. Griffin, High-resolution magic-angle-spinning NMR spectra of protons in deuterated solids, *J. Magn. Reson.* **98,** 408–413 (1992).
11. L. Zheng, K. W. Fishbein, R. G. Griffin, and J. Herzfeld, Two-dimensional solid-state ^{1}H NMR and proton exchange, *J. Am. Chem. Soc.* **115,** 6254–6261 (1993).
12. A. McDermott, T. Polenova, A. Böckmann, K. W. Zilm, E. K. Paulsen, R. W. Martin, and G. T. Montelione, Partial assignments for uniformly (^{13}C, ^{15}N)-enriched BPTI in the solid state, *J. Biomol. NMR* **16,** 209–219 (2000).
13. J. Pauli, B. vanRossum, H. Förster, H. J. M. deGroot, and H. Oschkinat, Sample optimization and identification of signal patterns of amino acid side chains in 2D-RFDR spectra of the α-spectrin SH3 domain, *J. Magn. Reson.* **143,** 411–416 (2000).
14. A. Abragam, "Principles of Nuclear Magnetism," Vol. 32, Clarendon Press, Oxford (1961).
15. A. E. Bennett, C. M. Rienstra, M. Auger, K. V. Lakshmi, and R. G. Griffin, Heteronuclear decoupling in rotating solids, *J. Chem. Phys.* **103,** 6951–6958 (1995).
16. M. Ernst, S. Bush, A. C. Kolbert, and A. Pines, Second-order recoupling of chemical-shielding and dipolar-coupling tensors under spin decoupling in solid-state NMR, *J. Chem. Phys.* **105,** 3387–3397 (1996).
17. M. Ernst, H. Zimmermann, and B. H. Meier, A simple model for heteronuclear spin decoupling in solid-state NMR, *Chem. Phys. Lett.* **317,** 581–588 (2000).
18. A. E. Bennett, J. H. Ok, R. G. Griffin, and S. Vega, Chemical shift correlation spectroscopy in rotating solids: Radio-frequency dipolar recoupling and longitudinal exchange, *J. Chem. Phys.* **96,** 8624–8627 (1992).
19. A. E. Bennett, C. M. Rienstra, J. M. Griffiths, W. Zhen, P. T. Lansbury, Jr., and R. G. Griffin, Homonuclear radio frequency-driven recoupling in rotating solids, *J. Chem. Phys.* **108,** 9463–9479 (1998).
20. J. Schaefer, R. A. McKay, and E. O. Stejskal, Double-cross-polarization NMR of solids, *J. Magn. Res.* **34,** 443–447 (1979).
21. C. P. Jaroniec, B. A. Tounge, J. Herzfeld, and R. G. Griffin, Frequency selective heteronuclear dipolar recoupling in rotating solids: Accurate ^{13}C–^{15}N distance measurements in uniformly ^{13}C, ^{15}N-labeled peptides, *J. Am. Chem. Soc.* **123,** 3507–3519 (2001).
22. P. J. Carroll, P. L. Stewart, and S. J. Opella, Structures of two model peptides: N-acetyl-D, L-valine and N-acetyl-L-valyl-L-leucine, *Acta Crystallogr. Sect. C* **46,** 243–246 (1990).
23. M. Ottiger, A. Bax, An empirical correlation between amide deuterium isotope effects on ^{13}Cα chemical shifts and protein backbone conformation, *J. Am. Chem. Soc.* **119,** 8070–8075 (1997).
24. S. O. Smith, K. Aschheim, and M. Groesbeek, Magic angle spinning NMR spectroscopy of membrane proteins, *Quart. Rev. Biophys.* **29,** 395–449 (1996).
25. S. J. Glaser, Coupling topology dependence of polarization-transfer efficiency in TOCSY and TACSY experiments, *J. Magn. Reson. A* **104,** 283–301 (1993).
26. C. M. Rienstra, M. E. Hatcher, L. J. Mueller, B. Sun, S. W. Fesik, and R. G. Griffin, Efficient multispin homonuclear double-quantum recoupling for magic-angle spinning NMR: ^{13}C–^{13}C correlation spectroscopy of U-^{13}C-erythromycin A, *J. Am. Chem. Soc.* **120,** 10602–10612 (1998).
27. C. M. Rienstra, M. Hohwy, L. J. Mueller, C. P. Jaroniec, B. Reif, and R. G. Griffin, Determination of multiple torsion angle constraints in U-^{13}C, ^{15}N-labeled peptides: 3D ^{1}H–^{15}N–^{13}C–^{1}H dipolar chemical shift NMR spectroscopy in rotating solids, submitted for publication.
28. A. E. McDermott, F. Creuzet, R. G. Griffin, L. E. Zawadzke, Q. Z. Ye, and C. T. Walsh, Rotational resonance determination of the structure of an enzyme-inhibitor complex—Phosphorylation of an (aminoalkyl)phosphonate inhibitor of D-alanyl-D-alanine Ligase by ATP, *Biochem.* **29,** 5767–5775 (1990).
29. F. Creuzet, A. McDermott, R. Gebhard, K. Vanderhoef, M. B. Spijkerassink, J. Herzfeld, J. Lugtenburg, M. H. Levitt, and R. G. Griffin, Determination of membrane-protein structure by rotational resonance NMR–bacteriorhodopsin, *Science* **251,** 783–786 (1991).
30. L. K. Thompson, A. E. McDermott, J. Raap, C. M. Vanderwielen, J. Lugtenburg, J. Herzfeld, and R. G. Griffin, Rotational resonance NMR-study of the active site in bacteriorhodopsin—conformation of the schiff-base linkage, *Biochemistry* **34,** 7931–7938 (1992).
31. A. E. McDermott, F. Creuzet, R. Gebhard, K. Vanderhoef, M. H. Levitt, J. Herzfeld, J. Lugtenburg, and R. G. Griffin, Determination of the internuclear distances and the orientation of functional-groups by solid-state NMR—Rotational resonance study of the conformation of retinal in bacteriorhodopsin, *Biochemistry* **33,** 6129–6136 (1994).
32. P. T. Lansbury-Jr., P. R. Costa, J. M. Griffiths, E. J. Simon, M. Auger, K. Halverson, D. A. Kocisko, A. S. Hendsch, T. T. Ashburn, R. G. S. Spenser, B. Tidor, and R. G. Griffin, Structural model for the β-amyloid fibril based on interstrand alignment of an antiparallel-sheet comprising a C-terminal peptide, *Nat. Struct.Biol.* **2,** 990–998 (1995).
33. T. L. S. Benzinger, D. M. Gregory, T. S. Burkoth, H. Miller-Auer, G. G. Lynn, R. E. Botto, and S. C. Meredith, Propagating structure of Alzheimer's β-amyloid(10–35) is parallel beta-sheet with residues in exact register, *Proc. Natl. Acad. Sci. USA* **95,** 13407–13412 (1998).
34. T. L. Benzinger, D. M. Gregory, T. S. Burkoth, H. Miller-Auer, D. G. Lynn, R. E. Botto, and S. C. Meredith, Two-dimensional structure of beta-amyloid(10–35) fibrils, *Biochemistry* **39,** 3491–3499 (2000).
35. K. Nomura, K. Takegoshi, T. Terao, K. Uchida, and M. Kainosho, Determination of the complete structure of a uniformly labeled molecule by rotational resonance solid-state NMR in the tilted rotating frame, *J. Am. Chem. Soc.* **121,** 4064–4065 (1999).
36. K. Nomura, K. Takegoshi, T. Terao, K. Uchida, and M. Kainosho, Three-dimensional structure determination of a uniformly labeled molecule by frequency-selective dipolar recoupling under magic-angle spinning, *J. Biomol. NMR* **17,** 111–123 (2000).
37. N. C. Nielsen, H. Bildsøe, H. J. Jacobsen, and M. H. Levitt, Double-quantum homonuclear rotary resonance: efficient dipolar recovery in

magic-angle spinning nuclear magnetic resonance, *J. Chem. Phys.* **101,** 1805–1812 (1994).

38. Y. K. Lee, N. D. Kurur, M. Helmle, O. G. Johannessen, N. C. Nielsen, and M. H. Levitt, Efficient Dipolar Recoupling in the NMR of rotating solids. A sevenfold symmetric radiofrequency pulse sequence, *Chem. Phys. Lett.* **242,** 304–309 (1995).

39. B. Reif, M. Hohwy, C. P. Jaroniec, C. M. Rienstra, and R. G. Griffin, NH–NH vector correlation in peptides by solid state NMR, *J. Magn. Reson.* **145,** 132–141 (2000).

40. S. Hafner and H. W. Spiess, Advanced solid-state NMR spectroscopy of strongly dipolar coupled spins under fast magic angle spinning, *Concepts Magn. Reson.* **10,** 99–128 (1998).

41. C. Filip, S. Hafner, I. Schnell, D. E. Demco, and H. W. Spiess, Solid-state nuclear magnetic resonance spectra of dipolar-coupled multi-spin systems under fast magic angle spinning, *J. Chem. Phys.* **110,** 423–440 (1999).

42. A. Wokaun and R. R. Ernst, Selective detection of multiple quantum transitions in NMR by two-dimensional spectroscopy, *Chem. Phys. Lett.* **52,** 407–412 (1977).